IL NUOVO CIMENTO **41 C** (2018) 93
DOI 10.1393/ncc/i2018-18093-8

Colloquia: IFAE 2017

THGEM: A fast growing MPGD technology

Fulvio Tessarotto(*)
INFN, Sezione di Trieste - Trieste, Italy

received 21 April 2018

Summary. — Thick-GEMs (THGEMs) are simple and robust gaseous multipliers, derived from the GEM design and proposed for large-scale applications. Classical THGEMs consist of Printed Circuit Boards (PCBs) with a regular pattern of holes obtained by drilling; they are manufactured by industry in large series and large size; their response for different geometrical parameters and operational conditions has been extensively studied. Different substrates (ceramic, glass, PTFE, etc.) and various production procedures have also been investigated with promising results. Different design options, like highly segmented electrodes, and different architectures, in particular those based on the Thick-WELL design are being actively studied. THGEMs are used as gaseous multipliers and as reflective photocathodes for VUV photons when coated with a CsI layer. THGEM-based Photon Detectors have been successfully implemented in 2016 on COMPASS RICH-1 for a total active area of 1.4 m^2. Applications of THGEM (also called LEM) technology in the field of cryogenic detectors, in particular for double-phase large volume Ar ones are proposed. The recently discovered phenomenon of bubble assisted electro-luminescence in liquid Xe opens the way to local dual phase cryogenic detector configurations when using THGEMs. The detection of X-rays and neutrons using THGEM-based devices is a very active field. Promising results have been obtained using THGEMs for imaging applications.

1. – Introduction

The field of Micro-Pattern Gaseous Detectors (MPGDs) today represents a dynamically growing sector of technologies, among which Thick Gas Electron Multipliers (THGEMs) are promising candidates for future large scale use and wide-spread applications.

This article summarizes the main characteristics of THGEMs, their variety in terms of substrate materials, geometries, production techniques, detector architecture and the specific challenges of different applications. Particular attention is reserved to the hybrid

(*) E-mail: `fulvio.tessarotto@ts.infn.it`

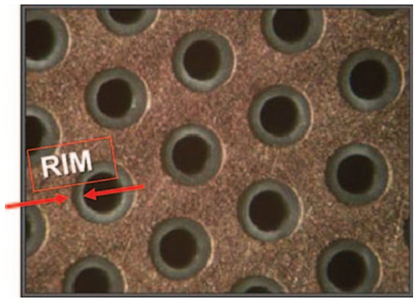

Fig. 1. – Image of a classical THGEM with the array of holes produced by drilling on a standard PCB.

THGEM + Micromegas Photon Detectors (PDs) recently installed on the RICH-1 Detector of the COMPASS Experiment at CERN and to the proposed large scale THGEM applications in the field of cryogenic detectors.

2. – THGEMs

Gas Electron Multiplies (GEMs) [1] consist of thin (50 μm), metal clad polyimide foils, with a high density matrix of holes, produced by chemical etching. Inserted between a drift and a collection electrode and properly biased, they provide proportional multiplication of the ionization electrons produced in the drift region and efficient transfer of electrons into the collection region. The multiplication occurs mainly inside the holes of the GEM, the readout electrode is physically independent from the GEM and the signal is fast, being generated by the movement of electrons. GEMs are presently used in many physics experiments and for a wide range of applications. Due to the flexible nature of the polyimide foils, GEMs need to be properly stretched on rigid mechanical supports or frames.

THGEMs are gaseous electron multipliers derived from the GEM design, scaling the geometrical parameters and changing the production technology: standard Printed Circuit Boards (PCBs) are used instead of the Cu-coated polyimide foils and the holes are obtained by drilling. They were introduced in parallel by several groups [2-6].

THGEMs are mechanically stiff and self-supporting, electrically robust and cost effective; they have typical thickness of 0.2–1.2 mm, cylindrical holes with diameter in the 0.2–1.0 mm range and pitch of 0.4–2.0 mm. Their holes can be provided with a rim, a clearence ring in the Cu layers around the holes which can vary from 0.0 to 0.2 mm in width. They can be industrially manufactured in large series and large size using standard PCB drilling and etching techniques (see fig. 1).

The space resolution provided by THGEM-based detectors is modest ($\sim$1 mm) [7] compared to the GEM case, and the material budget is larger, but the electron collection and transport is more effective [8] (for THGEMs the electron transverse diffusion is smaller than the hole diameter) and the achievable gains are higher [9, 10].

THGEMs with different geometrical parameters have been extensively characterized and their role as electron multipliers and as reflective photocathode has been studied in detail [11-14]. A special role is played by the rim: the maximum achievable gain increases exponentially with the rim size [11] but large gain variations over time and significant gain dependance on the irradiation history [15, 16] are seen for large rim THGEMs.

Apart from standard THGEMs, produced from PCB material, special THGEMs

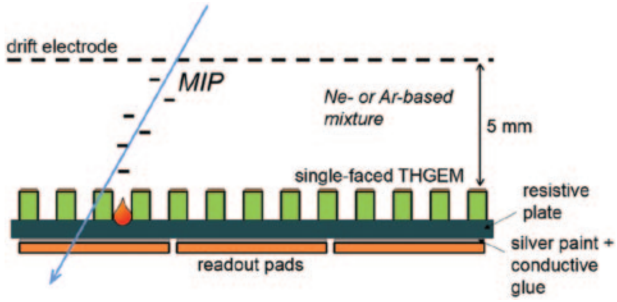

Fig. 2. – Scketch of an RPWELL proposed for large hadron calorimeters.

have been produced using different substrate materials, including noble substrates (ceramic [17], glass [18,19]), organic substrates (Kevlar, PTFE [20], PET, Arlon, etc.) or using different production procedures, including water jet or laser drilling and chemical etching.

THGEMs can be treated to have the holes covered by highly isolating films (polyurethane) or the electrodes covered by resistive layers: a particularly intense investigation of this design, called RETGEM (PCBs covered with resisitive kapton layers) has been performed [21].

Interesting THGEMs with different structures have been produced, in particular the Blind-THGEM, also called WELL [22], namely a THGEM with a closed bottom anode. The Resistive-Plate WELL (RPWELL) [23] is a novel gaseous multiplier based on the WELL concept: it consists of a single-sided copper-clad THGEM coupled to a segmented readout anode (pads or strips) through a thin high bulk-resistivity ($\sim 10^8$–$10^{10}\,\Omega$cm) plate (see fig. 2). It demonstrated discharge-free operation at high gas-avalanche gains and over a broad ionization range [24]; it is proposed for future large digital hadron calorimeters.

A THGEM electrode can be segmented in narrow strips allowing direct detection of THGEM signals from the strips without using a separate anode readout system.

The THCOBRA [25] is a THGEM having one of the faces equipped with additional anode strips winding between circular cathode strips (see fig. 3, top right). Primary avalanches occurring within the holes are followed by additional ones at the anode-strips vicinity. This double-avalanche structure allows for efficient collection by the cathode strips of the positive ions generated in the second avalanche [26]: this property, called Ion Back-Flow (IBF) suppression, is a key element of the electrical stability of gaseous multipliers operated at high gain. An evolution of the THCOBRA concept, the 2D-THCOBRA has the other face segmented in strips orthogonal to the COBRA strips (see fig. 3, bottom right): it is used as both electron multiplier and 2-D position sensitive readout element.

The technology for Capillary Plates (CP) production, typically used in vacuum-based PDs, also provides rigid electron multipliers in gas which could be included in the THGEM category. A CP is a plate made of a bundle of fine glass capillaries fused together; a CP used as a hole-type MPGD [27] has metallic electrodes deposited on both surfaces. CPs have been used for gaseous Photon Detectors [28] coupled to Micromegas [29], also with the capillaries inclined [30] to achieve further reduction of the IBF. A recent development of funnel glass CP allows achieving 83% of surface area opening, and thus a higher photoelectron collection efficiency for semitransparent photocathode PDs [31].

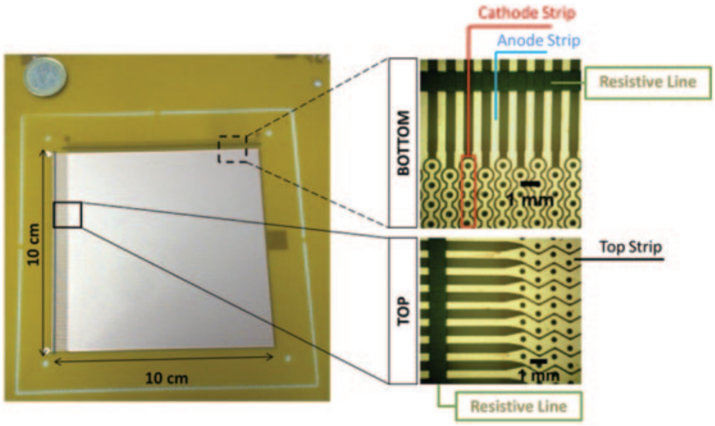

Fig. 3. – The THCOBRA and its strips.

THGEMs are often cascaded in multilayer architectures to provide higher stable gains, in detectors used or proposed for various applications, involving the detection of charged particles, UV or visible photons, X or γ-Rays and neutrons.

3. – THGEM-based Photon Detectors

The need of covering large area of efficient detectors of single photons at affordable costs triggered the development of gaseous photon detectors in the 1980's and 1990's; the THGEM technology has recently allowed to improve the performance of gaseous PDs in the UV region and to investigate their application for visible photon detection too.

Chambers hosting multilayer standard THGEMs arrangements with CsI coating on the top of the first THGEM [11] have been built and operated in Ar-based and in Ne-based gas mixtures [32, 33] and they were proposed for the VHMPID project of the ALICE Experiment at the LHC.

High gain, stable operation in laboratory and at test beam lines [34] have been achieved using small-size prototypes of various configurations, in particular with triple identical THGEMs, the first one being CsI-coated: effective gain in the range of 10^5–10^6 [35] are commonly achieved, and time resolutions below 10 ns [36] are typical.

Obtaining the same performance in terms of gain and stability with large or medium size ($300 \times 300\,\mathrm{cm}^2$) triple THGEM PDs is more challenging: a dedicated R&D program [13, 37] investigating the origin of non-uniformity of the detector response and the spark rates as well as the performance of different PD configurations provided a specific procedure for large area THGEM production [38], quality assessment and configuration optimization. An investigation of the IBF [39], which in a standard triple THGEM configuration approaches 30%, showed that it can be reduced by a complete misalignment of the holes in different layers and using unbalanced values of the electric field in the transfer regions between THGEMs.

To achieve a further IBF suppression an alternative architecture of the PD combining Micromegas and THGEM technologies was tested and provided better results in terms of performance and stability for large area prototypes [40]. This hybrid configuration has been chosen for the upgrade of the RICH-1 detector of the COMPASS Experiment at CERN SPS, which has been equipped in 2016 with four new MPGD-based PDs [41], covering a total active area of $1.4\,\mathrm{m}^2$ and replacing MWPC-based PDs which were in

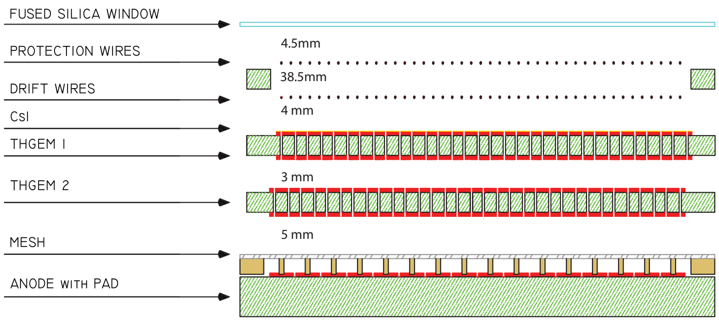

Fig. 4. – Sketch of the hybrid single photon detector: two THGEM layers are coupled to a bulk Micromegas. The image is not to scale.

operation since 2002. This upgrade is particularly interesting because for the first time MPGD-based detectors of single photons have been used in a running experiment. The detector architecture [42] consists of a combination (see fig. 4) of two THGEMs, the first acting as reflective photocathode, and a Micromegas on a pad segmented anode.

Each hybrid PD covers a $600 \times 600\,\mathrm{mm}^2$ active area and is formed by two identical modules ($600 \times 300\,\mathrm{mm}^2$), arranged side by side. Two planes of wires are used to shape the electric field in the drift region. All THGEMs (fig. 5, left) have the same geometrical parameters: they are $470\,\mu$m thick ($400\,\mu$m dielectric and $2 \times 35\,\mu$m Cu), their holes have $400\,\mu$m diameter, $800\,\mu$m pitch and no rim. The electrodes are segmented in 24 mm wide strips and the voltage bias is individually provided to each sector of the THGEMs. The THGEMs used as photocathodes were coated by Ni-Au and by a 300 nm thick CsI photoconverting layer (see fig. 5, right).

The two THGEM layers are mounted at a distance of 3 mm, in a configuration of complete hole misalignment, to achieve the maximum charge spread; 5 mm separate the middle THGEM from the Micromegas, which were produced at CERN using the bulk technology procedure [43, 44]. The square anode pads facing the Micromegas mesh have 8 mm pitch and are biased at positive voltage; the mesh, which is the only non-segmented electrode, is kept at ground potential. Each anode pad receives the biasing voltage via an individual $470\,\mathrm{M}\Omega$ resistor.

The signal is transmitted from the anode pad via capacitive coupling to a readout pad facing it, buried inside the anode PCB (at $70\,\mu$m distance from the anode pad) and connected to the front-end. The resistive-capacitive pad scheme dumps the effects of discharges and protects the front-end electronics [45], which is based on the APV25 chip.

COMPASS hybrid PDs operate with an Ar/CH_4 50/50 gas mixture at typical effective gain values of few 10^4; the IBF to the photocathode is $\sim 3\%$. They show good operational stability and efficient detection of single photons.

The detection of Cherenkov light in the visible range brings several advantages with respect to the UV case: larger photon yield, better angular resolution wider range of optical media with good transparency, including silica aerogel and larger tolerance to contaminants.

Combining these advantages with the opportunities offered by gaseous PDs (cost-effectiveness for large area, low material budget, magnetic insensibilty) is extremely appealing and a large R&D effort is being invested in developing the visible-light gaseous PD technology.

Due to the high chemical reactivity and the fragility of visible light photoconverters it

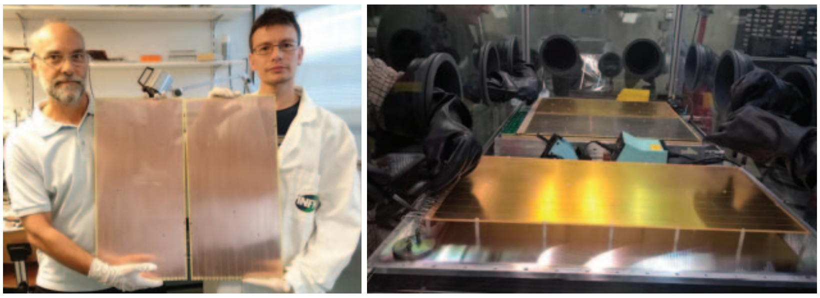

Fig. 5. – THGEMs before CsI coating (left) and after coating, being mounted on a COMPASS hybrid PD inside a glove-box (right).

is a challenging task to use them in gaseous detectors: most of the commonly used materials are incompatible with them, the ion-induced secondary electron emission is copious and their aging by ion bombardment is fast. Coating photocathodes with protective films seriously reduces their QE [46].

GEM-based gaseous PDs with bialkali photocathodes have been built and tested in sealed mode operation [47, 48], with an ion-blocking gate [49] or incorporating a Micro-Hole and Strip Plate (MHSP) into a Multi-GEM cascaded multiplier [50, 51]. The polyimide GEMs material seems however to be incompatible with visible light photocathodes [52].

Good compatibility is instead seen when using MPGDs made of Pyrex glass plates and treated by sand micro-blasting, coupled with a Micromegas [53, 54].

4. – Cryogenic applications and scintillation imaging

High, stable electron multiplication in noble gases and liquids at cryogenic temperatures were achieved for the first time when GEM-based detectors, called CRyogenic Avalanche Detectors (CRAD) [55] were introduced. Triple GEM detectors provided gains approaching 10^4 [56] opening the possibility to develop of a dual-phase CRAD equipped with CsI photocathode, able to detect both the charge ionization signal and the primary scintillation signals from liquid Ar (LAr) [57].

The use of THGEMs, (also called large Electron Multipliers: LEMs) was soon proposed [58] in view of giant LAr scintillation, Cherenkov and charge imaging experiment; THGEMs were indeed tested to be as effective as GEMs [59] for cryogenic applications [60, 61].

THGEMs made of PTFE (Polytetrafluoroethylene) are particularly suited for cryogenic low noise applications because of their radiopurity [20].

A wide variety of THGEM-based detectors have been proposed and tested [62]: they can be divided into three classes:

- detectors performing photon conversion and charge multiplication in a gas separated by a window from the pure noble liquid (or gas) of the cryogenic detector.
- detectors operated directly in the noble gas of a dual-phase cryogenic detector.
- detectors immersed in the cryogenic noble liquid.

An example belonging to the first class is the Gaseous PhotoMultiplier (GPM) [63] formed by a triple THGEM (each having thickess = 0.4 mm, hole diameter = 0.4 mm, hole pitch = 0.8 mm, rim = 50 μm) with active diameter of 100 mm, held 2 mm apart, with CsI on the first one, operated in Ne/CH_4, coupled through a UV window to a small dual-phase LXe TPC. It allows to record signals over a high dynamic range (from single photons to massive electroluminescence signals) in the same operating conditions, with maximal gain above 10^5, assuring high photon detection efficiency and stable operation.

A member of the second class is the dual-phase CRAD prototype [64] consisting of four THGEMs ($10 \times 10\,\mathrm{cm}^2$), two horizontally immersed in the LAr at 48 mm distance, biased to form a drift region in the liquid which covered the second THGEM by 4 mm, forming an electron emission region. A double-THGEM assembly with the first THGEM acting as the anode was placed 18 mm above the liquid surface, to form an electroluminescence gap and provide multiplication. A matrix of GAPDs and a set of cryogenic PMTs with wavelength shifters registered the scintillation light. A systematic study of the proportional electroluminescence was performed. A recent measurement [65] showed that a small ($\sim$50 ppm) N_2 doping level of the Ar enhances the CRAD sensitivity to the proportional electroluminescence signal.

A representative of the third class is the Liquid Hole Multiplier [66], proposed as a cascade of THGEMs (or analogous hole multipliers) with CsI photocathodes deposited on their surfaces, immersed in the noble liquid. Photoelectrons from primary scintillation or ionization electrons are focused into the electrode holes and give origin to electroluminescence in the intense electric field in the liquid inside the holes; the amplification of the UV photons in the cascaded THGEM structure could result in detectable signals. Liquid Xe proportional electroluminescence in THGEM holes was indeed observed [67] and its large intensity attributed to the possible presence of bubbles (local dual-phase conditions) near the THGEM holes [68], which have recently been directly observed [69]. The possibility to exploit this phenomenon in large-volume local dual-phase liquid TPCs is fascinating.

Scintillation proportional counters [70] exploit the photon emission process induced by electron-molecule collisions; this emission can be so copious to allow the use of external optical imaging.

A two-dimensional detector with high spatial resolution can be established by incorporating an imaging element, such as a charge-coupled device (CCD), detecting the scintillation light produced during the charge amplification process. High resolution X-ray images can be obtained [71] with low integration time using a glass-GEM multiplier in CF_4, thanks to the CF_4 strong scintillation component in the visible range (500 nm–700 nm), which matches the spectral sensitivity of CCD cameras. Similar techniques are very promising for wide range X-Ray imaging applications.

A triple GEM detector operating in ^{3}He-CF_4 gas mixtures [72], suitable for thermal neutron detection, has provided detailed images of the tracks resulting from the interaction between thermal neutrons and the ^{3}He atom. Recently a glass THGEM combined with a micro-structured ^{10}B foil and a mirror-lens-CCD system [73] has been used for neutron imaging.

MPGD-based scintillating imaging detectors have extraordinary potential, could find application in many different fields outside physics research and help advancement in novel detector invention.

5. – Conclusions

A large effort to refine and consolidate THGEM technologies is taking place, exploring new ideas, new techniques and new applications. Large hybrid THGEM-Micromegas

PDs, covering 1.4 m^2 are successfully operated since 2016 on the COMPASS RICH-1 detector. Developments in the dynamic fields of cryogenic detectors and scintillation light imaging are continuous and new projects are proposing the use of THGEM technologies.

REFERENCES

[1] Sauli F., *Nucl. Instrum. Methods A*, **386** (1997) 531.
[2] Jeanneret P., PhD Thesis, Neuchâtel University (2001).
[3] Periale L. *et al.*, *Nucl. Instrum. Methods A*, **478** (2002) 377.
[4] Ostling J. *et al.*, *IEEE Trans. Nucl. Sci.*, **50** (2003) 809.
[5] Barbeau P. S. *et al.*, *IEEE Trans. Nucl. Sci.*, **50** (2003) 1285.
[6] Chechik R. *et al.*, *Nucl. Instrum. Methods A*, **535** (2004) 303.
[7] Cortesi M. *et al.*, *J. Instrum.*, **2** (2007) P09002.
[8] Chechik R. *et al.*, *Nucl. Instrum. Methods A*, **553** (2004) 35.
[9] Shalem C. *et al.*, *Nucl. Instrum. Methods A*, **558** (2006) 475.
[10] Shalem C. *et al.*, *Nucl. Instrum. Methods A*, **558** (2006) 468.
[11] Breskin A. *et al.*, *Nucl. Instrum. Methods A*, **598** (2009) 107.
[12] Alexeev M. *et al.*, *Nucl. Instrum. Methods A*, **623** (2010) 129.
[13] Alexeev M. *et al.*, *J. Instrum.*, **7** (2012) C02014.
[14] Rocco E., *Development of a gaseous photon detector for Cherenkov imaging applications*, PhD Thesis, Turin University (2010) CERN-THESIS-2010-053.
[15] Alexeev M. *et al.*, *Nucl. Instrum. Methods A*, **610** (2009) 174.
[16] Alexeev M. *et al.*, *J. Instrum.*, **10** (2014) P03026.
[17] Xie Y. *et al.*, *Nucl. Instrum. Methods A*, **729** (2013) 809.
[18] Takahashi H. *et al.*, *Nucl. Instrum. Methods A*, **724** (2013) 1.
[19] Mitsuya Y. *et al.*, *Nucl. Instrum. Methods A*, **795** (2015) 156.
[20] Xie W. Q. *et al.*, *Chin. Phys. C*, **37** 11 (2013) 116001.
[21] Oliveira R. *et al.*, *Nucl. Instrum. Methods A*, **576** (2007) 362.
[22] Arazi L. *et al.*, *J. Instrum.*, **7** (2012) C05011.
[23] Rubin A. *et al.*, *J. Instrum.*, **8** (2013) P11004.
[24] Moleri L. *et al.*, *Nucl. Instrum. Methods A*, **845** (2017) 262.
[25] Amaro F. D. *et al.*, *J. Instrum.*, **5** (2010) P10002.
[26] Veloso J. F. C. A. *et al.*, *Nucl. Instrum. Methods A*, **639** (2011) 134.
[27] Sakurai H. *et al.*, *Nucl. Instrum. Methods A*, **374** (1996) 341.
[28] Peskov V. *et al.*, *Nucl. Instrum. Methods A*, **433** (1999) 492.
[29] Vavra J. and Sumiyoshi T., *Nucl. Instrum. Methods A*, **535** (2004) 334.
[30] Vavra J. and Sumiyoshi T., *Nucl. Instrum. Methods A*, **553** (2004) 76.
[31] Sugiyama H. *et al.*, *Nucl. Instrum. Methods A* (2016).
[32] Peskov V. *et al.*, *J. Instrum.*, **5** (2010) P11004.
[33] Peskov V. *et al.*, *Nucl. Instrum. Methods A*, **695** (2012) 154.
[34] Alexeev M. *et al.*, *Nucl. Instrum. Methods A*, **732** (2013) 264.
[35] Alexeev M. *et al.*, *J. Instrum.*, **5** (2010) P03009.
[36] Alexeev M. *et al.*, *Nucl. Instrum. Methods A*, **695** (2012) 159.
[37] Alexeev M. *et al.*, *J. Instrum.*, **8** (2013) C12005.
[38] Alexeev M. *et al.*, *J. Instrum.*, **9** (2014) C03046.
[39] Alexeev M. *et al.*, *J. Instrum.*, **8** (2013) P01021.
[40] Alexeev M. *et al.*, *Nucl. Instrum. Methods A*, **824** (2016) 139.
[41] Alexeev M. *et al.*, *Status of COMPASS RICH-1 upgrade with MPGD-based photon detectors*, in *Proceedings of MPGD 2015 International Conference on Micro-Pattern Gaseous Detectors* (EDP Sciences) 2016.
[42] Alexeev M. *et al.*, *Nucl. Instrum. Methods A*, **876** (2017) 96.
[43] Giomataris I. *et al.*, *Nucl. Instrum. Methods A*, **560** (2006) 405.
[44] Bouchez J. *et al.*, *Nucl. Instrum. Methods A*, **574** (2007) 425.

[45] Abbon P. *et al.*, *Nucl. Instrum. Methods A*, **567** (2006) 104.
[46] Peskov V. *et al.*, *Nucl. Instrum. Methods A*, **348** (1994) 269.
[47] Balcerzyk M. *et al.*, *IEEE Trans. Nucl. Sci.*, **NS50** (2003) 847.
[48] Chechik R. *et al.*, *Nucl. Instrum. Methods A*, **502** (2003) 195.
[49] Breskin A. *et al.*, *Nucl. Instrum. Methods A*, **553** (2005) 46.
[50] Lyashenko A. *et al.*, *J. Instrum.*, **4** (2009) P07005.
[51] Breskin A. *et al.*, *Nucl. Instrum. Methods A*, **623** (2010) 318.
[52] Tokanai F. *et al.*, *Nucl. Instrum. Methods A*, **610** (2009) 164.
[53] Sumiyoshi T. *et al.*, *Nucl. Instrum. Methods A*, **639** (2011) 121.
[54] Moriya T. *et al.*, *Nucl. Instrum. Methods A*, **732** (2013) 269.
[55] Buzulutskov A. *et al.*, *IEEE Trans. Nucl. Sci.*, **NS50** (2003) 2491.
[56] Bondar A. *et al.*, *Nucl. Instrum. Methods A*, **556** (2006) 273.
[57] Bondar A. *et al.*, *Nucl. Instrum. Methods A*, **581** (2007) 241.
[58] Rubbia A., *Experiments for CP-violation: A giant liquid argon scintillation, Cerenkov and charge imaging experiment?* in *Proceedings of the II International Workshop on Neutrino Oscillations in Venice, Venice, Italy, December 2003*, arXiv:hep-ph/0402110.
[59] Bondar A. *et al.*, *J. Instrum.*, **3** (2008) P07001.
[60] Badertscher A. *et al.*, *Nucl. Instrum. Methods A*, **641** (2011) 48.
[61] Cantini C. *et al.*, *J. Instrum.*, **10** (2015) P03017.
[62] Buzulutskov A. *et al.*, *J. Instrum.*, **7** (2012) C02025.
[63] Arazi L. *et al.*, *J. Phys.: Conf. Ser.*, **650** (2015) 012010.
[64] Bondar A. *et al.*, *EPL*, **112** 1 (2015) 19001.
[65] Bondar A. *et al.*, *Nucl. Instrum. Methods A*, **845** (2016) 206.
[66] Breskin A. *et al.*, *J. Phys.: Conf. Ser.*, **460** (2013) 012020.
[67] Arazi L. *et al.*, *J. Instrum.*, **8** (2013) C12004.
[68] Arazi L. *et al.*, *J. Instrum.*, **10** (2015) P08015.
[69] Arazi L. *et al.*, *J. Instrum.*, **10** (2015) P11002.
[70] Charpak G. *et al.*, *Nucl. Instrum. Methods A*, **258** (1987) 177.
[71] Fujiwara T. *et al.*, *J. Instrum.*, **8** (2013) C12020.
[72] Fraga F. A. F. *et al.*, *Nucl. Instrum. Methods A*, **478** (2002) 357.
[73] Fujiwara T. *et al.*, *Nucl. Instrum. Methods A*, **838** (2016) 124.